The Variable Crab Nebula: Evidence for a Connection between GeV flares and Hard X-ray Variations

Colleen A. Wilson-Hodge[1], A.K. Harding, E.A. Hays[2], M. L. Cherry[3], G. L. Case[4], M. H. Finger[5], P. Jenke[6], X. Zhang[7]

[1]NASA's MSFC, [2]NASA/GSFC, [3]LSU, [4]La Sierra Univ., [5]USRA, [6]UAH, [7]MPE

Abstract

In 2010, hard X-ray variations (Wilson-Hodge et al. 2011) and GeV flares (Tavani et al 2011, Abdo et al. 2011) from the Crab Nebula were discovered. Connections between these two phenomena were unclear, in part because the timescales were quite different, with yearly variations in hard X-rays and hourly to daily variations in the GeV flares. The hard X-ray flux from the Crab Nebula has again declined since 2014, much like it did in 2008-2010. During both hard X-ray decline periods, the Fermi LAT detected no GeV flares, suggesting that injection of particles from the GeV flares produces the much slower and weaker hard X-ray variations. The timescale for the particles emitting the GeV flares to lose enough energy to emit synchrotron photons in hard X-rays is consistent with the yearly variations observed in hard X-rays and with the expectation that the timescale for variations slowly increases with decreasing energy. This hypothesis also predicts even slower and weaker variations below 10 keV, consistent with the non-detection of counterparts to the GeV flares by Chandra (Weisskopf et al 2013). We will present a comparison of the observed hard X-ray variations and a simple model of the decay of particles from the GeV flares to test our hypothesis.

Observations & Results

Introduction:
Is there a relationship between the GeV flares and the longer timescale flux variations seen in the hard X-rays?
During the two periods when the hard X-ray flux declines, 2008-2010 and 2014-2016, GeV flares are absent. The GeV flaring activity is more prevalent from 2010-2014, when the hard X-ray flux is increasing, suggesting that the GeV flares may be driving the changes in hard X-ray flux.

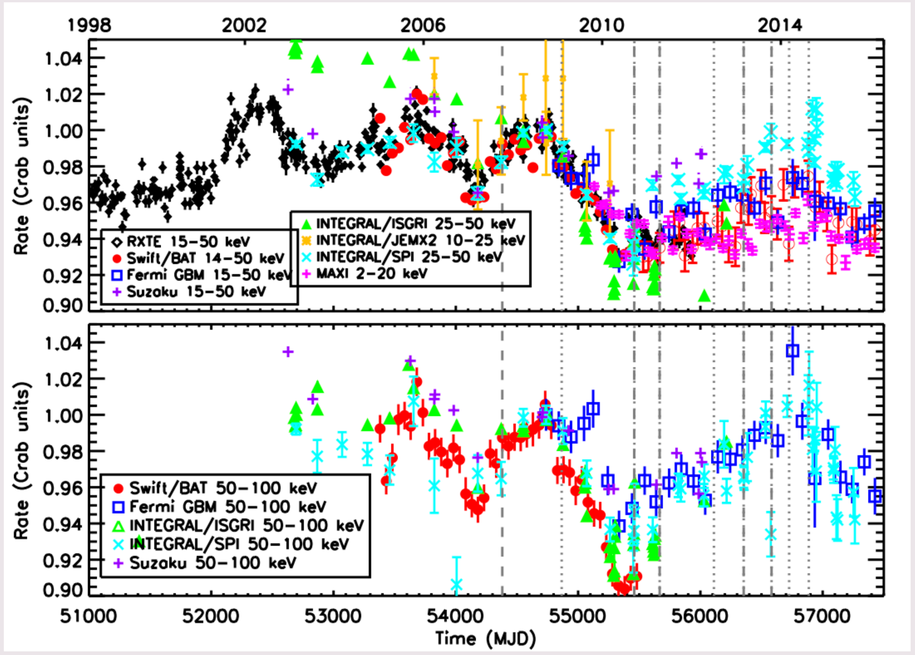

Figure 1: Composite Crab light curves from 1999-2016 for RXTE/PCA (15-50 keV - black diamonds), Swift/BAT (Top: 14-50 keV, Bottom: 50-100 keV - red filled circles), Fermi/GBM (Top 15-50 keV, Bottom:50-100 keV - blue open squares), INTEGRAL/SPI (Top: 25-50 keV, Bottom: 50-100 keV - light blue x's), INTEGRAL/ISGRI (Top: 25-50 keV, Bottom: 50-100 keV - green filled triangles), INTEGRAL/JEM-X2 (10-25 keV, gold asterisks), and MAXI (2-20 keV - magenta crosses). Each data set has been normalized to its mean rate in the time interval MJD 54690-54790. All error bars except Swift/BAT include only statistical errors. Times of high energy flares observed with AGILE (dashed lines) and Fermi LAT (dotted lines) are shown for reference. This figure is an extension of that presented in Wilson-Hodge et al. 2011, ApJ, 727, L40

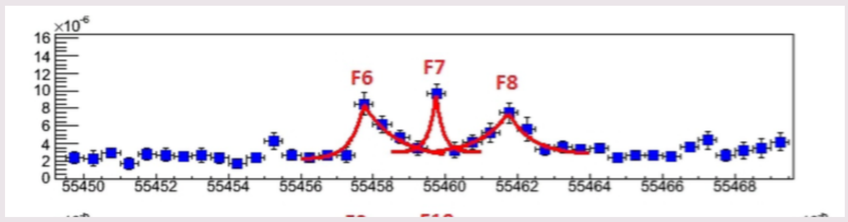

Figure 2: September 2010 LAT flare (LAT flux E>100 MeV (Striani et al. 2013). The table lists some of the observables from these flares, which include peak photon energy, peak emitted power, rise time and cooling time.

Typical N ~ (1 - 3) x 10^38(ΔΩ /4π)

	Name	MJD	τ_1 (hr)	τ_2 (hr)	Peak Flux	$B(mG)$	γ^* (10^9)	l (10^{15} cm)
2007 (AGILE)	F_1	54381.5	22 ± 11	10 ± 5	1000 ± 150	$1.0 - 2.0$	$2.6 - 4.8$	$1.2 - 3.6$
	F_2	54382.5	14 ± 7	6 ± 3	1400 ± 200	$1.1 - 2.1$	$2.3 - 4.3$	$0.8 - 2.2$
	F_3	54383.7	11 ± 5	14 ± 7	900 ± 150	$1.0 - 2.0$	$2.6 - 4.8$	$0.8 - 1.7$
2009 (FERMI)	F_4	54865.8	10 ± 5	20 ± 10	700 ± 140	$0.7 - 1.3$	$2.6 - 4.8$	$0.6 - 1.6$
	F_5	54869.2	10 ± 5	22 ± 11	830 ± 90	$0.8 - 1.4$	$2.6 - 4.8$	$0.6 - 1.6$
2010 (AGILE & FERMI)	F_6	55457.8	8 ± 4	22 ± 11	850 ± 130	$0.7 - 1.3$	$2.5 - 4.7$	$0.5 - 1.3$
	F_7	55459.8	6 ± 3	6 ± 3	1000 ± 100	$1.4 - 2.6$	$2.6 - 4.8$	$0.3 - 0.9$
	F_8	55461.9	19 ± 10	8 ± 4	750 ± 110	$0.8 - 1.4$	$2.5 - 4.8$	$0.9 - 3.1$
2011 (FERMI & AGILE)	F_9	55665.0	9 ± 5	9 ± 5	1480 ± 80	$1.2 - 2.2$	$2.8 - 5.0$	$0.5 - 1.5$
	F_{10}	55667.3	10 ± 5	24 ± 12	2200 ± 85	$1.3 - 2.3$	$2.7 - 4.9$	$0.6 - 1.6$

For each flare, shown in Figure 3 for LAT, we can derive a magnetic field, Lorentz factor, emission length scale (listed in Table 1), and number of emitting particles (Equation to the left), assuming a monochromatic particle distribution and Doppler factor = 1.

Using the derived particle distribution, and a simple model, we predict an emission light curve at lower energies, shown in Figure 4.

Model Predictions & Comparisons

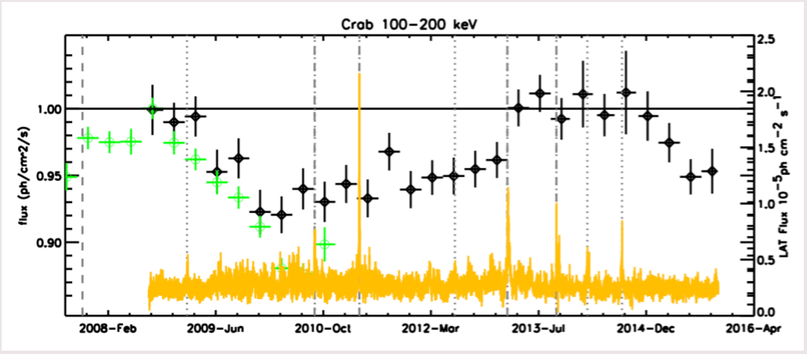

Figure 3: Swift/BAT and Fermi GBM fluxes (100-200 keV, 100-d averages) compared with the public LAT light curve (E>100 MeV, 1-day averages)

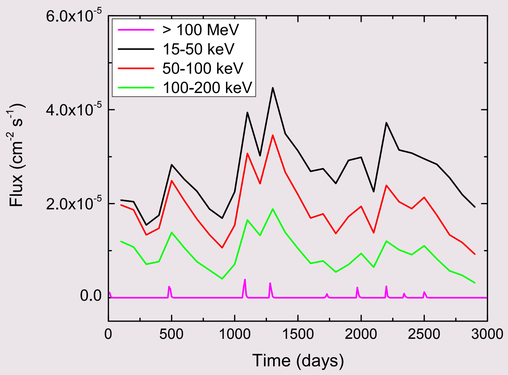

Figure 4: Predicted hard X-ray light Curves in 3 energy bands, 15-50 keV (top, black), 50-100 keV (center, red), and 100-200 keV (center, green). The magenta curve on the bottom shows the simple model for the GeV flares as delta functions.

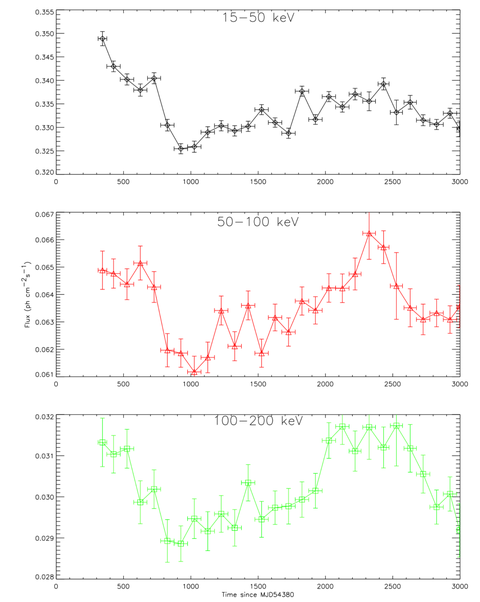

Figure 5: GBM Light Curves (100-day bins) in 3 energy bands, 15-50 keV (top, black), 50-100 keV (center, red), and 100-200 keV (bottom, green).

Summary & Conclusions

The general shape of the hard X-ray light curves (shown in Figures 3 & 5), especially in the 50-100 and 100-200 keV bands, is similar to the predicted light curve, starting from about 1000 days from 2007 GeV flare. The early parts of the light curve (before 1000 days since the first observed flare) do not match the predictions because there are most likely pre-2007 flares that we do not know about that would affect the light curve.

The predicted fluxes do not agree with the observed fluxes. The current model is very simplistic, treating the flares as delta functions, so improvements to the model may bring the fluxes into better agreement. More work is clearly needed to improve the model and understand the fluxes.

The simplistic model appears to predict the correct timescales for the observed hard X-ray variability. This is also interesting, because this model would also predict even longer timescales and lower amplitudes for soft X-ray variability, possibly explaining why multi wavelength campaigns have so far been unsuccessful (e.g. Weisskopf et. al 2013)

colleen.wilson@nasa.gov